AD-A124 323 PRELIMINARY ANALYSIS OF AN FM/CW SYSTEM OPERATING OVER A DISTRIBUTED FLAT.. (U) FLORIDA UNIV GAINESVILLE ENGINEERING AND INDUSTRIAL EXPERIMEN.. 1/1

UNCLASSIFIED P Z PEEBLES ET AL. JUN 82 HDL-CR-82-116-3 F/G 17/9 NL

END

FILMED

DTIC

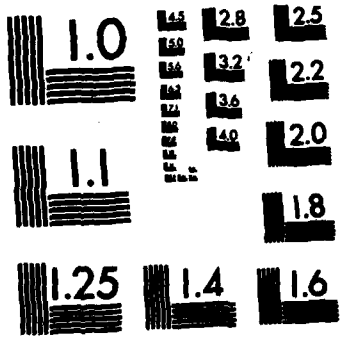

12

HDL-CR-82-116-3

Preliminary Analysis of an FM/CW System Operating Over A Distributed Flat-Surface Target

by Peyton Z. Peebles, Jr.

June 1982

Prepared by
The University of Florida
Engineering and Industrial
Experiment Station

Gainesville, FL 32611

Under contract
DAAK21-81-C-0116

U.S. Army Electronics Research and Development Command
Harry Diamond Laboratories
Adelphi, MD 20783

Approved for public release; distribution unlimited.

UNCLASSIFIED
SECURITY CLASSIFICATION OF THIS PAGE (When Data Entered)

REPORT DOCUMENTATION PAGE	READ INSTRUCTIONS BEFORE COMPLETING FORM
1. REPORT NUMBER: HDL-CR-82-116-3	2. GOVT ACCESSION NO.: AD-A124323
	3. RECIPIENT'S CATALOG NUMBER:
4. TITLE (and Subtitle): Preliminary Analysis of an FM/CW System Operating Over A Distributed Flat-Surface Target	5. TYPE OF REPORT & PERIOD COVERED: Contractor Report
	6. PERFORMING ORG. REPORT NUMBER:
7. AUTHOR(s): Peyton Z. Peebles, Jr. HDL Contact: J. Sichina	8. CONTRACT OR GRANT NUMBER(s): DAAK21-81-C-0116
9. PERFORMING ORGANIZATION NAME AND ADDRESS: Engineering and Industrial Experiment Station University of Florida Gainesville, FL 32611	10. PROGRAM ELEMENT, PROJECT, TASK AREA & WORK UNIT NUMBERS: Program element: 6.26.16.A HDL Proj: A18214
11. CONTROLLING OFFICE NAME AND ADDRESS: U. S. Army Materiel Development and Readiness Command Alexandria, VA 22333	12. REPORT DATE: June 1982 13. NUMBER OF PAGES: 29
14. MONITORING AGENCY NAME & ADDRESS (if different from Controlling Office): Harry Diamond Laboratories 2800 Powder Mill Road Adelphi, MD 20783	15. SECURITY CLASS. (of this report): UNCLASSIFIED 15a. DECLASSIFICATION/DOWNGRADING SCHEDULE:

16. DISTRIBUTION STATEMENT (of this Report)
Approved for public release; distribution unlimited.

17. DISTRIBUTION STATEMENT (of the abstract entered in Block 20, if different from Report)

18. SUPPLEMENTARY NOTES
Work Unit Title: Fuze Technology
DA-1L662616AH77, DRCMS Code: 662616.11.H7700

19. KEY WORDS (Continue on reverse side if necessary and identify by block number)
FM ranging systems
Frequency modulation
Continuous-wave receivers
Distributed radar targets

20. ABSTRACT (Continue on reverse side if necessary and identify by block number)
The power spectrum of the intermediate-frequency (IF) output of an FM/cw system is found when the system is operating over a flat surface. General equations for a homogeneous surface are derived and a specific example is worked out in detail for vertically incident systems.

DD FORM 1 JAN 73 1473 EDITION OF 1 NOV 65 IS OBSOLETE

UNCLASSIFIED
SECURITY CLASSIFICATION OF THIS PAGE (When Data Entered)

CONTENTS

FIGURES

1. INTRODUCTION

In recent times considerable knowledge has been gathered that relates to both the methods of processing signals and the performance that results when an FM/cw system (radar) operates with a point target. The simplest systems use a single down-conversion receiver (or the envelope detector equivalent receiver) and sense the resulting Doppler signal. More sophisticated systems use intermediate frequency (IF) references for a second down-conversion (or correlation) operation; these references can be either simple sinewaves or "functional references" designed to maximize system response for an anticipated specific target range. These correlation operations can even be combined with other signal processing operations to produce a system sensitive to the direction of the Doppler (incoming versus outgoing target). Other techniques exist for controlling system response versus target range and even reducing undesirable range sidelobes. In most cases the analysis of these advanced systems has been developed only for point targets.

Many practical applications of FM/cw radars call for the system to operate above the earth's surface. In fact, the surface may actually be the radar's target. For example, an FM/cw radar functioning as a fuzing device may be required to sense when the radar has reached a specific height above the surface so as to detonate its charge. In this case the surface backscatter from directly below the radar contains the most important information. However, backscattered power from other directions now becomes important because the surface is extended and is not a point target. Analysis of system performance becomes more difficult with extended targets and the available knowledge base is not as well developed as for point targets, even for simple systems.

In this report we examine the response of a relatively simple form of FM/cw radar when moving toward a homogeneous flat extended (earth) surface. The assumption of homogeneity does not prevent us from considering various types of surfaces, such as grassy fields, water, etc.; it only prevents us from mixing the types.

The system response that is studied is the output (Doppler) signal from a simple down-conversion system that uses a functional reference. The power spectrum of the response is found and the form of the reference is specified that "optimizes" the power spectrum.

Results found herein are considered preliminary in that they represent only the initial findings of an ongoing study.

In the development of our principal results for the distributed surface it is helpful to first formulate the single, or point, target problem in a way that will establish a particular viewpoint.

2. POINT TARGET CASE

Two principal purposes are served by initially formulating the point target problem: we are able to define the geometry of the problem in a way that allows relatively easy transition to the extended surface analysis, and we can formulate analysis procedures to determine the form of the "optimum" signal processor. These procedures are similar in the extended surface analysis.

The problem's geometry is defined in figure 1. The FM/cw system is instantaneously located at an altitude h above a flat surface which is the xy plane. The system is moving with speed V along a trajectory with an angle of incidence θ_V, defined as the angle between the flight path and the vertical (z axis). At an appropriate later time the system would impact at point I. The point scatterer, or target, is located at point S in the xy plane. Target location is defined by its position (r_i, θ_i, ϕ_i) in spherical coordinates located with origin at the FM/cw system at point R. For the purposes of this section, i has only the single value unity. However, we use the notation so that additional scatterers may be introduced in the next section.

We define the complex transmitted signal of the FM/cw system as

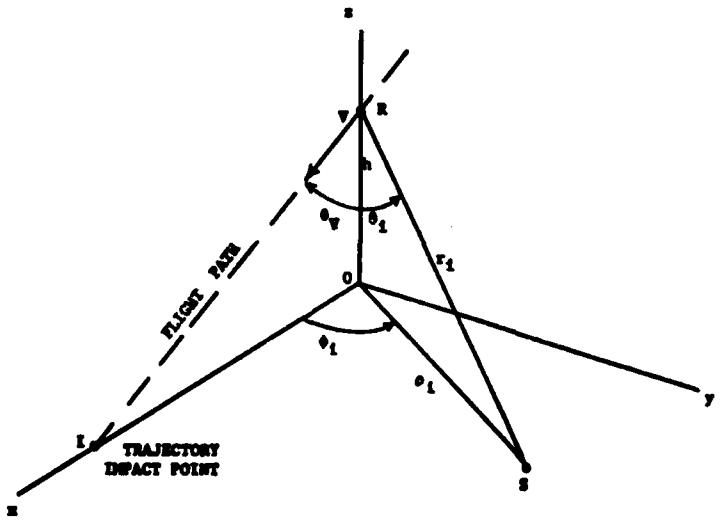

Figure 1. Geometry for FM/cw system located at point R and a scatterer at point S.

$$v_T(t) \triangleq V_T e^{j\omega_0 t + j\beta(t)} , \tag{1}$$

where

$$V_T \triangleq \text{peak signal amplitude} , \tag{2}$$

$$j \triangleq \sqrt{-1} , \tag{3}$$

$$\omega_0 \triangleq \text{transmitted carrier angular frequency,} \tag{4}$$

$$\beta(t) \triangleq D \int_{-\infty}^{t} m(\xi)d\xi , \tag{5}$$

$$D \triangleq \text{modulator's constant (rad/s-V),} \tag{6}$$

$$m(t) \triangleq \text{modulation message.} \tag{7}$$

We also make the following additional definitions:

$$G_T(\theta_i, \phi_i) \triangleq \text{transmit antenna one-way voltage pattern in direction } (\theta_i, \phi_i), \tag{8}$$

$$G_R(\theta_i, \phi_i) \triangleq \text{receive antenna one-way voltage pattern in direction } (\theta_i, \phi_i), \tag{9}$$

$$\sigma_i \triangleq \text{cross section of scatterer at point S .} \tag{10}$$

The system of interest is assumed to have the form shown in figure 2 where the indicated waveforms are the complex ones for analysis. The actual system waveforms are the real parts of the complex signals. The reference signal that serves as the local oscillator for the receive-path mixer is assumed to have the arbitrary form

$$v_{ref}(t) \triangleq Z(t)e^{j\omega_0 t} , \tag{11}$$

where Z(t) is an arbitrary complex envelope

$$Z(t) \triangleq A(t)e^{jB(t)} . \tag{12}$$

We seek to find A(t) and B(t) so that the response $v_{IF}(t)$ is optimum in an appropriate sense.

The system IF output can be shown to be

$$v_{IF}(t) = \frac{V_T \lambda G_T^*(\theta_i, \phi_i) G_R^*(\theta_i, \phi_i)\sqrt{\sigma_i}}{(4\pi)^{3/2} r_i^2} A(t)e^{j2\omega_0 r_i/c + jB(t) - j\beta\left(t - \frac{2r_i}{c}\right)} , \tag{13}$$

where c is the speed of light in free space.

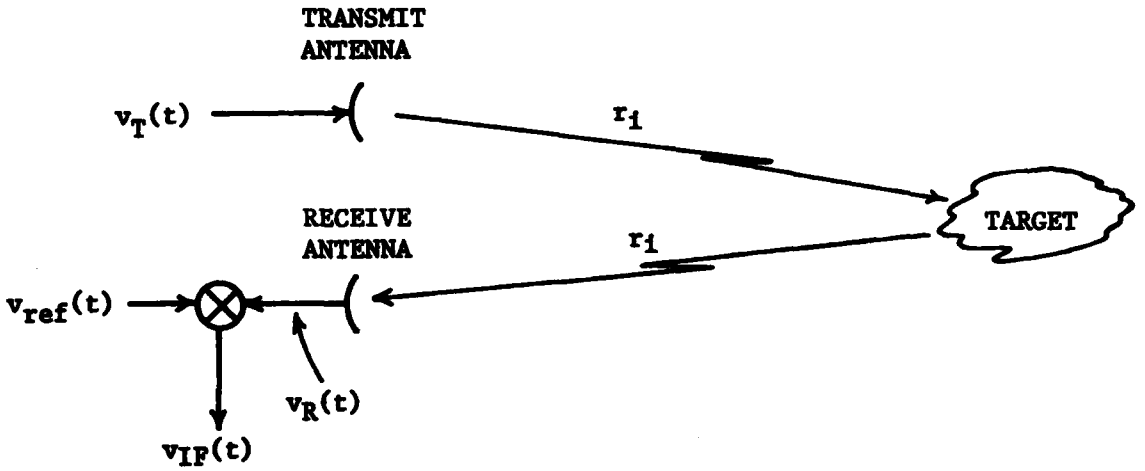

Figure 2. Form of FM/cw system that uses an arbitrary reference signal.

Next we assume that, over the signal processing time of interest, r_i can be approximated by the first two terms in its series expansion:

$$r_i(t) \approx r_{0i} - \dot{r}_i t \ , \tag{14}$$

where

$$r_{0i} \triangleq \text{constant (value of } r_i \text{ at } t = 0) \tag{15}$$

and

$$\dot{r}_i \triangleq \left.\frac{dr_i(t)}{dt}\right|_{t=0} . \tag{16}$$

Thus,

$$2\omega_0 r_i/c \approx (2\omega_0 r_{0i}/c) - (2\omega_0 \dot{r}_i/c)t \tag{17}$$

$$\triangleq \omega_0 \tau_{0i} - \omega_{di} t \ , \tag{18}$$

where

$$\tau_{0i} \triangleq 2r_{0i}/c \tag{19}$$

$$\omega_{di} \triangleq 2\omega_0 \dot{r}_i/c \ . \tag{20}$$

If we now assume that target motion affects mainly the return signal's phase but has little affect on the complex envelope (low-frequency modulations), then (13) becomes

$$v_{IF}(t) = \frac{V_T \lambda G_T^*(\theta_i, \phi_i) G_R^*(\theta_i, \phi_i) \sqrt{\sigma_i}}{(4\pi)^{3/2} r_i^2} A(t) e^{j\omega_0 \tau_{0i} - j\omega_{di} t + jB(t) - j\beta(t - \tau_{0i})} . \tag{21}$$

The principal purpose of our analysis shall be to find the power spectrum of the IF output. In an ideal case this spectrum should contain a single pair of impulses at the Doppler angular frequencies $\pm \omega_{di}$. The power spectrum is computed by Fourier transforming the time-average of the IF signal's autocorrelation function. The autocorrelation function of the real part of (21) is

$$R_{IF}(t, t + \varepsilon) = \frac{V_T^2 G_T^2(\theta_i, \phi_i) G_R^2(\theta_i, \phi_i) \lambda^2 \sigma_i}{2(4\pi)^3 r_i^4} A(t) A(t + \varepsilon) \Big\{$$

$$\cos\left[-\omega_{di}\varepsilon + B(t + \varepsilon) - B(t) - \beta(t + \varepsilon - \tau_{0i}) + \beta(t - \tau_{0i})\right]$$

$$+ \cos\left[2\omega_0 \tau_{0i} - 2\omega_{di} t - \omega_{di}\varepsilon + B(t) + B(t + \varepsilon)\right. \tag{22}$$

$$\left. - \beta(t - \tau_{0i}) - \beta(t + \varepsilon - \tau_{0i})\right] \Big\} .$$

In writing (22) the antenna patterns have been assumed to be real functions No generality is lost in this assumption because the only change in (22) for the general case is the subtraction of twice the phase angle of $G_T(\theta_i, \phi_i)G_R(\theta_i, \phi_i)$ from the argument of the second cosine term, and, as will result, the second term is nearly zero when the time average is formed and the optimum reference is found.

We form the time average of (22) for periodic modulations and note that the second term will nearly always be small because of rapid cycling of the cosine factor due to the term $2\omega_{di}t$ in its argument. We therefore get:

$$R_{IF}(\varepsilon) \triangleq A\left\{R_{IF}(t, t+\varepsilon)\right\} = \frac{V_T^2 G_T^2(\theta_i, \phi_i) G_R^2(\theta_i, \phi_i)\lambda^2\sigma_i}{2(4\pi)^3 r_i^4} \operatorname{Re}\left\{ \right.$$

$$\left. \frac{1}{T}\int_{-T/2}^{T/2} A(t)A(t+\varepsilon)e^{jB(t+\varepsilon)-j\beta(t+\varepsilon-\tau_{0i})-jB(t)+j\beta(t-\tau_{0i})}dt\, e^{-j\omega_{di}\varepsilon}\right\} . \tag{23}$$

Now for a given τ_{0i} and prescribed $\beta(t)$, the Fourier transform of (23) will possess impulses at $\pm\omega_{di}$ only if the integral is independent of ε. Furthermore, the "strength" of the impulses will be largest if the integral is maximized. Since

$$\int_a^b f(x)dx \le \int_a^b |f(x)|dx , \tag{24}$$

the integral (23) is maximized by first selecting B(t) so that the exponent is zero for all ε:

$$B(t) = \beta(t - \tau_{0i}) . \tag{25}$$

The integral is then further maximized by choosing

$$A(t) = \text{constant} . \tag{26}$$

The "optimum" reference for the system to use for a point target at range delay τ_{0i} is therefore

$$Z(t) = A(t)e^{jB(t)} = e^{j\beta(t-\tau_{0i})} , \tag{27}$$

where we select A(t) = constant = 1 for convenience.

With the optimum Z(t) we have

$$R_{IF}(\varepsilon) = \frac{V_T^2 G_T^2(\theta_i, \phi_i) G_R^2(\theta_i, \phi_i) \lambda^2 \sigma_i}{2(4\pi)^3 r_i^4} \cos(\omega_{di}\varepsilon) \tag{28}$$

$$S_{IF}(\omega) = \frac{V_T^2 G_T^2(\theta_i, \phi_i) G_R^2(\theta_i, \phi_i) \lambda^2 \sigma_i \pi}{2(4\pi)^3 r_i^4} [\delta(\omega - \omega_{di}) + \delta(\omega + \omega_{di})] . \tag{29}$$

Thus, the power spectrum possesses the desired impulses at the Doppler angular frequency.

3. DISTRIBUTED FLAT-SURFACE TARGET

To develop the distributed target problem we shall first represent the surface as a finite collection of discrete scatterers having random, statistically independent phase angles, uniformly distributed on $(0, 2\pi)$. The number of scatterers is then allowed to become infinite to form a continuous surface. Summations present in the autocorrelation function of the IF output signal become integrals.

For a finite number of scatterers the IF signal now becomes a sum of terms like (21) provided scatterer cross sections are properly interpreted. To make the subsequent transition to a continuum of scatterers direct, we make the following substitution:

$$\sqrt{\sigma_i} \rightarrow \sqrt{d\sigma_i}\, e^{j\gamma_i} , \tag{30}$$

where $d\sigma_i$ is the cross section of the small (differential) scatterer i that has the random phase angle γ_i. Cross section $d\sigma_i$ will equal the product of σ_0, the cross section per unit area that is typical of the surface type, and the scatterer's differential scattering area, dA_i, in the xy plane:

$$d\sigma_i = \sigma_0 dA_i = \sigma_0 r_i^2 \tan\theta_i \, d\theta_i d\phi_i . \tag{31}$$

In general, σ_0 is a function of the angle of the incident wave that causes scattering. Thus,

$$\sigma_0 = \sigma_0(\theta_i) , \tag{32}$$

a function of θ_i.

By substituting (30, (31) and (32) into (21) the IF output becomes

$$v_{IF}(t) = \sum_{\text{all } i} \frac{V_T \lambda G_T^*(\theta_i, \phi_i) G_R^*(\theta_i, \phi_i) \sqrt{d\sigma_i}}{(4\pi)^{3/2} r_i^2} A(t) e^{-j\gamma_i - j\omega_{di}t + j\beta(t) - j\beta(t-\tau_{0i})} \tag{33}$$

The autocorrelation function of the real part of (33) is found to be

$$R_{IF}(t,\ t+\varepsilon) = E[\mathrm{Re}\ \{v_{IF}(t)\}\ \mathrm{Re}\ \{v_{IF}(t+\varepsilon)\}]$$

$$= \frac{V_T^2\lambda^2}{2(4\pi)^3}\ \mathrm{Re}\left\{\sum_{\text{all } i}\frac{G_T^2(\theta_i,\ \phi_i)G_R^2(\theta_i,\ \phi_i)}{r_i^4}A(t)A(t+\varepsilon)d\sigma_i\right. \tag{34}$$

$$\left.\cdot\, e^{-jB(t)+jB(t+\varepsilon)-j\omega_{di}\varepsilon-j\beta(t+\varepsilon-\tau_{0i})+j\beta(t-\tau_{0i})}\right\},$$

where $E[\cdot]$ stands for the statistical expectation operation. Next, we drop subscripts i and allow the sum to become an integral using (31). The integral involves only angles θ and ϕ, however, because scattering patch distance r must be restricted such that the scatterer lies in the xy plane. This location is preserved by substituting

$$r = h/\cos\ \theta \tag{35}$$

$$\tau_0 = \frac{2r}{c} = \frac{2h}{c\ \cos\ \theta}\ . \tag{36}$$

We get

$$R_{IF}(t,\ t+\varepsilon) = \frac{V_T^2\lambda^2}{2(4\pi)^3h^2}\ \mathrm{Re}\left\{A(t)A(t+\varepsilon)e^{-jB(t)+jB(t+\varepsilon)}\right.$$

$$\cdot\int_{\theta=0}^{\pi/2}\sigma_0(\theta)\ \sin\ \theta\ \cos\ \theta\int_{\phi=0}^{2\pi}G_T^2(\theta,\ \phi)G_R^2(\theta,\ \phi)e^{-j\omega_{dx}\varepsilon\sin\theta\cos\phi}d\phi \tag{37}$$

$$\left.\cdot\, e^{j\omega_{dh}\varepsilon\cos\theta-j\beta(t+\varepsilon-\tau_0)+j\beta(t-\tau_0)}d\theta\right\},$$

where the radial Doppler angular frequency, ω_d, of any differential scattering patch is related to its components, ω_{dh} and ω_{dx}, in the h and x directions, respectively (see figure 1), by

$$\omega_d = \omega_{dh}\ \cos\ \theta + \omega_{dx}\ \sin\ \theta\ \cos\varepsilon\ \phi\ , \tag{38}$$

with

$$\omega_{dh} \triangleq (2\omega_0V/c)\ \cos\ \theta_V \tag{39}$$

$$\omega_{dx} \triangleq (2\omega_0V/c)\ \sin\ \theta_V\ . \tag{40}$$

3.1 Selection of Reference Signal for Periodic Modulations

Our ultimate goal is to find the power spectrum of the IF output signal; it is the Fourier transform of the time average of the autocorrelation function (37). As in the point target case we seek to make this time average as independent of ε and as large as possible. The only factor of (37) involved in the time average is

$$A\left\{A(t)A(t+\varepsilon)e^{-jB(t)+j\beta(t-\tau_0)+jB(t+\varepsilon)-j\beta(t+\varepsilon-\tau_0)}\right\}_{T/2} = \frac{1}{T}\int_{-T/2} A(t)A(t+\varepsilon)e^{-jB(t)+j\beta(t-\tau_0)+jB(t+\varepsilon)-j\beta(t+\varepsilon-\tau_0)}dt \quad . \tag{41}$$

This integral will be independent of ε and maximum when

$$B(t) = \beta(t-\tau_0) \tag{42}$$

$$A(t) = \text{constant}. \tag{43}$$

We see that the optimum holds for only one value of τ_0 [from (36) this means only one value of θ]. With the optimum $A(t)$ and $B(t)$ (41) becomes

$$\text{Time Average} = \frac{1}{T}\int_{-T/2}^{T/2} e^{-j\beta\left(t-\frac{2h}{c\cos\theta_0}\right)+j\beta\left(t-\frac{2h}{c\cos\theta}\right)} \cdot e^{j\beta\left(t+\varepsilon-\frac{2h}{c\cos\theta_0}\right)-j\beta\left(t+\varepsilon-\frac{2h}{c\cos\theta}\right)}dt \quad , \tag{44}$$

where θ_0 is the angle at which optimization occurs.

To reduce (44) further we consider periodic modulations with fundamental angular frequency ω_T. Now because the modulation $m(t)$ is periodic by assumption, the quantity $\exp\{j\beta(t+\varepsilon) - j\beta(t)\}$ is also periodic with the same period and will have a Fourier series defined by

$$e^{j\beta(t+\varepsilon)-j\beta(t)} = \sum_{n=-\infty}^{\infty} C_n(\varepsilon)e^{jn\omega_T t} \quad , \tag{45}$$

where

$$\boxed{C_n(\varepsilon) = \frac{1}{T}\int_{-T/2}^{T/2} e^{j\beta(t+\varepsilon)-j\beta(t)-jn\omega_T t}dt \quad .} \tag{46}$$

On substitution of (46) into (44) a simplified form is found for the required time average, which, when used in (37), allows the time-averaged autocorrelation function, denoted by $R_{IF}(\varepsilon)$, to be written in the form

$$R_{IF}(\varepsilon) = \frac{V_T^2 \lambda^2}{2(4\pi)^3 h^2} \sum_{n=-\infty}^{\infty} |C_n(\varepsilon)|^2 \int_{\theta=0}^{\pi/2} \sigma_0(\theta) \cos\theta \sin\theta \int_{\phi=0}^{2\pi} G_T^2(\theta, \phi) G_R^2(\theta, \phi) \cdot \cos\left\{\omega_{dh}\varepsilon \cos\theta + \omega_{dx}\varepsilon \sin\theta \cos\phi - n\omega_T \frac{2h}{c}\left[\frac{1}{\cos\theta} - \frac{1}{\cos\theta_0}\right]\right\} d\phi d\theta \, . \tag{47}$$

It appears unlikely that (47) can be solved analytically for arbitrary patterns and arbitrary surface scattering function $\sigma_0(\theta)$. Therefore, in the remainder of this report we seek to simplify (47) in order to obtain tractable results.

3.2 Constant Antenna Patterns

The two integrals in (47) are intimately coupled through the transmit and receive pattern functions. We may decouple the integrals to a great extent by assuming the patterns are constants over the angles of interest. Thus,

$$G_T(\theta, \phi) \approx G_{T0} \tag{48}$$

$$G_R(\theta, \phi) \approx G_{R0} \, .$$

For many FM/cw systems these assumptions are reasonable.

By substituting (48) and (49) into (47) and making use of a known integral[1] we may obtain

$$R_{IF}(\varepsilon) = \frac{V_T^2 \lambda^2 G_{T0}^2 G_{R0}^2 \pi}{(4\pi)^3 h^2} \sum_{n=-\infty}^{\infty} |C_n(\varepsilon)|^2 \int_{\theta=0}^{\pi/2} \sigma_0(\theta) \cos\theta \sin\theta \cdot J_0(\omega_{dx}\varepsilon \sin\theta) \cos\left\{\omega_{dh}\varepsilon \cos\theta - n\omega_T \frac{2h}{c}\left[\frac{1}{\cos\theta} - \frac{1}{\cos\theta_0}\right]\right\} d\theta \, . \tag{50}$$

The computation of (50) and the subsequent Fourier transformation to obtain the IF power spectrum can be done by computer. However, even for relatively simple functions that represent $\sigma_0(\theta)$, (50) is difficult to solve analytically

---

[1] M. Abramowitz and I. A. Stegun (editors), Handbook of Mathematical Functions with Formulas, Graphs, and Mathematical Tables (p 360, #9.1.21).

in a manner that leads to readily interpreted expressions.† In order to obtain at least one analytical solution to (50) we shall make one additional simplifying assumption.

4. VERTICAL INCIDENCE

If the FM/cw system is vertically incident on the flat surface, $\theta_V = 0$, and therefore $\omega_{dx} = 0$. The autocorrelation function (50) can now be reduced further. If we define functions $S_{C_n}(\omega)$ and $I_n(\omega)$ by

$$S_{C_n}(\omega) \triangleq F_\varepsilon\{|C_n(\varepsilon)|^2\} \tag{51}$$

$$I_n(\omega) = F_\varepsilon\left\langle \int_0^{\pi/2} \sigma_0(\theta) \cos\theta \sin\theta \cos\left\{\omega_{dh}\varepsilon \cos\theta - n\omega_T \frac{2h}{c}\left[\frac{1}{\cos\theta} - \frac{1}{\cos\theta_0}\right]\right\} d\theta \right\rangle , \tag{52}$$

where $F_\varepsilon\{\cdot\}$ represents taking the Fourier transform with respect to ε, the power spectrum, denoted by $S_{IF}(\omega)$, which is the Fourier transform of (50), becomes

$$S_{IF}(\omega) = F_\varepsilon\{R_{IF}(\varepsilon)\} = \frac{V_T^2 \lambda^2 G_{T0}^2 G_{R0}^2 \pi}{(4\pi)^3 h^2} \sum_{n=-\infty}^{\infty} \frac{1}{2\pi} \int_{-\infty}^{\infty} S_{C_n}(\xi) I_n(\omega - \xi) d\xi \ . \tag{53}$$

In obtaining (53) use is made of the fact that the transform of the product of two "time" functions is $1/2\pi$ times the convolution of their two spectra[2].

For our assumed problem where m(t) is periodic we have $|C_n(\varepsilon)|^2$ periodic in ε so that it has a Fourier series defined by

$$|C_n(\varepsilon)|^2 = \sum_{k=-\infty}^{\infty} E_{kn} e^{jk\omega_T \varepsilon} \ , \tag{54}$$

where

$$E_{kn} = \frac{1}{T} \int_{-T/2}^{T/2} |C_n(\varepsilon)|^2 e^{-jk\omega_T \varepsilon} d\varepsilon \ . \tag{55}$$

---

[2] Peyton Z. Peebles, Jr., Probability, Random Variables, and Random Signal Principles, McGraw-Hill, 1980 (p 249).

† Solutions in terms of multiple infinite series expansions can be obtained but interpretation of results is difficult.

The Fourier transform, or spectrum, of $|C_n(\varepsilon)|^2$ becomes

$$S_{C_n}(\omega) \triangleq F_\varepsilon\{|C_n(\varepsilon)|^2\} = 2\pi \sum_{k=-\infty}^{\infty} E_{kn}\delta(\omega - k\omega_T) \ . \tag{56}$$

On substituting (56) into (53) we have

$$S_{IF}(\omega) = \frac{V_T^2\lambda^2 G_{T0}^2 G_{R0}^2 \pi}{(4\pi)^3 h^2} \sum_{n=-\infty}^{\infty} \sum_{k=-\infty}^{\infty} E_{kn} I_n(\omega - k\omega_T) \ . \tag{57}$$

Clearly, $S_{IF}(\omega)$ is made up of shifted replicas of $I_n(\omega)$ centered at multiples of ω_T. If we assume

$$|\omega_{dh}| \leq \omega_T/2 \ , \tag{58}$$

these replicas do not overlap in frequency. Furthermore, we are mainly interested in the frequency region $|\omega| \leq \omega_T/2$ so that only the term for k = 0 in (57) is most important; if we denote by $S_{\omega_d}(\omega)$ the (Doppler region) part of $S_{IF}(\omega)$ in the region $|\omega| \leq \omega_T/2$, then for $|\omega| \leq \omega_{dh}$, it becomes

$$S_{\omega_d}(\omega) = \frac{V_T^2\lambda^2 G_{T0}^2 G_{R0}^2 \pi}{(4\pi)^3 h^2} \left\{ E_{00} I_0(\omega) + \sum_{n=1}^{\infty} \left[E_{0n} I_n(\omega) + E_{0(-n)} I_{-n}(\omega) \right] \right\} \ . \tag{59}$$

Now from (46)

$$C_{-n}(\varepsilon) = e^{-jn\omega_T\varepsilon} C_n(-\varepsilon) \ , \tag{60}$$

so

$$|C_{-n}(\varepsilon)|^2 = |C_n(-\varepsilon)|^2 \tag{61}$$

and

$$|E_{0(-n)}|^2 = |E_{0n}|^2 \tag{62}$$

from (55). It only remains to evaluate $I_n(\omega)$ and $I_{-n}(\omega)$ to reduce (59) to a final form.

It is shown in the appendix that (52) will reduce to

---

[2] Peyton Z. Peebles, Jr., Probability, Random Variables, and Random Signal Principles, McGraw-Hill, 1980 (p 256).

$$I_n(\omega) = \int_0^{\pi/2} \sigma_0(\theta) \cos\theta \sin\theta \left\{ \pi e^{-jn\omega_T \frac{2h}{c}\left[\frac{1}{\cos\theta} - \frac{1}{\cos\theta_0}\right]} \delta(\omega - \omega_{dh}\cos\theta) + \pi e^{jn\omega_T \frac{2h}{c}\left[\frac{1}{\cos\theta} - \frac{1}{\cos\theta_0}\right]} \delta(\omega + \omega_{dh}\cos\theta) \right\} d\theta$$

$$= \frac{\pi|\omega|}{\omega_{dh}^2} \sigma_0\left[\cos^{-1}\left(\frac{|\omega|}{\omega_{dh}}\right)\right] \begin{cases} e^{-jn\omega_T \frac{2h}{c}\left[\frac{\omega_{dh}}{|\omega|} - \frac{1}{\cos\theta_0}\right]}, & 0 < \omega < \omega_{dh} \\ e^{jn\omega_T \frac{2h}{c}\left[\frac{\omega_{dh}}{|\omega|} - \frac{1}{\cos\theta_0}\right]}, & -\omega_{dh} < \omega < 0 \\ 0, & \omega_{dh} < |\omega| \end{cases} \quad (63)$$

Finally, we may use (63) and (62) in (59) to obtain the IF output signal's power spectrum in the Doppler region:

$$S_{\omega_d}(\omega) = \frac{V_T^2 \lambda^2 G_{T0}^2 G_{R0}^2 \pi^2}{(4\pi)^3 h^2 \omega_{dh}^2} |\omega| \sigma_0\left[\cos^{-1}\left(\frac{|\omega|}{\omega_{dh}}\right)\right] \cdot \left\{ E_{00} + 2\sum_{n=1}^{\infty} E_{0n} \cos\left[n\omega_T \frac{2h}{c}\left(\frac{\omega_{dh}}{|\omega|} - \frac{1}{\cos\theta_0}\right)\right] \right\}, \quad |\omega| < \omega_{dh}, \quad (64)$$

where

$$E_{0n} = \frac{1}{T} \int_{-T/2}^{T/2} |C_n(\varepsilon)|^2 d\varepsilon . \quad (65)$$

Several observations can be made relative to (64). First, the factor $|\omega|$ will be maximum for $|\omega| = \omega_{dh}$ because $S_{\omega_d}(\omega)$ must be zero for $|\omega| > \omega_{dh}$. Second, it is typical that the scattering function $\sigma_0(\cdot)$ is largest for vertical incidence when its argument is zero, the case here where $|\omega| = \omega_{dh}$. Therefore, the factor $\sigma_0[\cos^{-1}(|\omega|/\omega_{dh})]$ also helps maintain $S_{\omega_d}(\omega)$ maximum at $|\omega| = \omega_{dh}$. Furthermore, $\sigma_0[\cdot]$ is a dominant term in controlling the shape of $S_{\omega_d}(\omega)$. The faster $\sigma_0(\cdot)$ decreases with its argument, the faster $S_{IF}(\omega)$ decreases from its maximum for $|\omega|$ smaller than ω_{dh}. Third, we note that all $E_{0n} \geq 0$ so that all the cosine terms in (64) add in phase, producing a maximum value, when $|\omega| = \omega_{dh}$ if we select $\cos\theta_0 = 1$, or $\theta_0 = 0$. Behavior of the sum of cosines will depend on the choice of modulation function through $C_n(\varepsilon)$ and the sum's value is difficult to estimate. However, as $|\omega|$

decreases below ω_{dh} the terms involving higher values of n begin to cycle rapidly so that $S_{\omega_d}(\omega)$ is expected to have rapid ripples in its amplitude as $|\omega|$ approaches zero.

4.1 Exponential Scattering Surfaces

As an example to illustrate the behavior of (64) assume $\sigma_0(\theta)$ is given by

$$\sigma_0(\theta) = ae^{-b\tan\theta}, \tag{66}$$

where $a > 0$ and $b > 0$ are constants. This function is not too unrealistic because it is a reasonable fit to published data. For $b \approx 1.4$ it fits data for terrain forested by trees about 50-ft high when measured at X band.[3] Other data,[4] for sea surfaces with winds from 10 to 20 knots when measured at frequencies near L band, are approximated by (66) when $b \approx 8.2$.

With $\theta_0 = 0$, (66) becomes

$$\sigma_0 \cos^{-1}[(|\omega|/\omega_{dh})] = ae^{-b\sqrt{\left(\frac{\omega_{dh}}{\omega}\right)^2 - 1}} \tag{67}$$

while (64) reduces to

$$S_{\omega_d}(\omega) = \frac{V_T^2 \lambda^2 G_{T0}^2 G_{R0}^2 \pi^2 a}{(4\pi)^3 h^2 \omega_{dh}^2} |\omega| e^{-b\sqrt{\left(\frac{\omega_{dh}}{\omega}\right)^2 - 1}} \left\{ E_{00} + 2 \sum_{n=1}^{\infty} E_{0n} \cos\left[n\omega_T \frac{2h}{c}\left(\frac{\omega_{dh}}{|\omega|} - 1\right)\right]\right\}, \quad |\omega| < \omega_{dh}, \tag{68}$$

$$= 0, \qquad |\omega| > \omega_{dh}.$$

The precise values of (68) depend on the coefficients E_{0n} which, in turn, depend on the modulation employed. Because of this fact, only the general behavior of $S_{\omega_d}(\omega)$ can be estimated. Based on earlier comments pertaining to (64) a rough sketch of how (68) might behave is shown in figure 3.

4.2 Sawtooth Modulation

Additional evaluation of (68) requires the modulation be specified. For a sawtooth FM that sweeps a band B(Hz) in T seconds and instantaneously repeats sweeps repetitively, it can be shown that

---

[3] M. I. Skolnik, Introduction to Radar Systems, McGraw-Hill, 1962 (p 525).

[4] M. I. Skolnik, Introduction to Radar Systems, McGraw-Hill, 2nd Edition, 1980 (p 475).

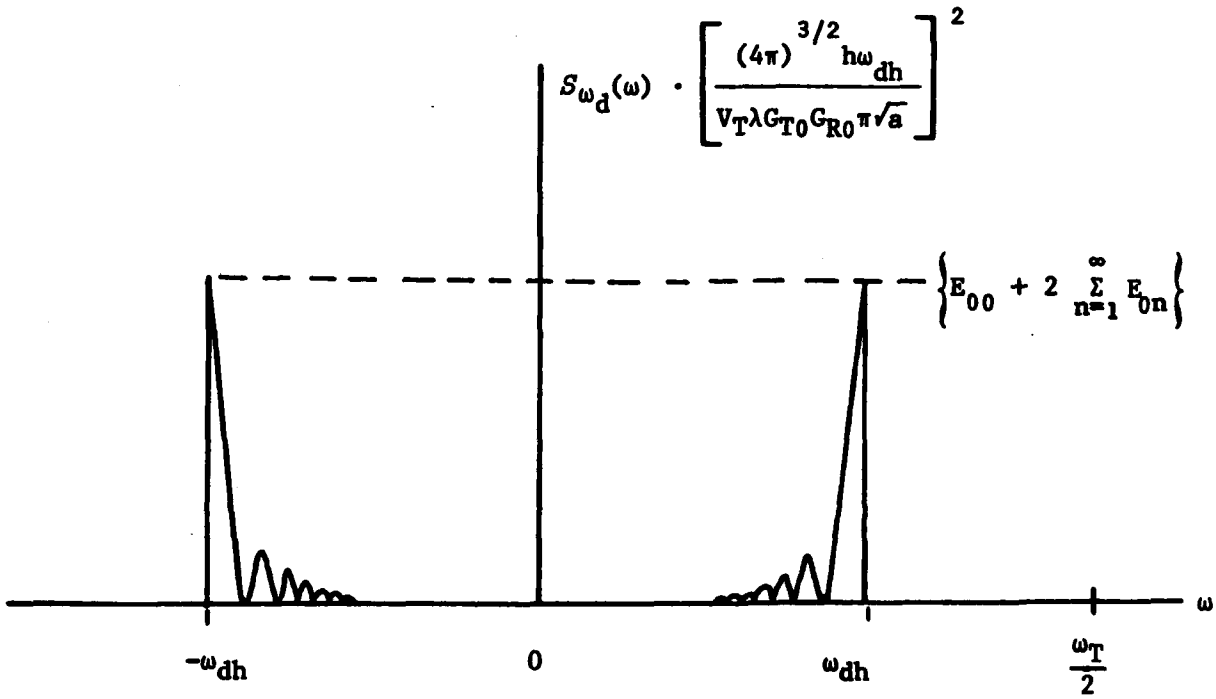

Figure 3. Rough plot of $S_{\omega_d}(\omega)$ when the FM/cw system has constant antenna patterns and vertical incidence over a flat surface with exponential scattering characteristic.

$$C_n(\varepsilon) = \left(\frac{BT - \bar{\varepsilon}}{BT}\right) Sa\left\{\pi(\bar{\varepsilon} - n)\left(\frac{BT - \bar{\varepsilon}}{BT}\right)\right\} e^{j\pi[\bar{\varepsilon}+n(\bar{\varepsilon}/BT)-n]}$$

$$+ (\bar{\varepsilon}/BT)Sa\{\pi(\bar{\varepsilon} - n - BT)\bar{\varepsilon}/BT\}e^{j\pi[\bar{\varepsilon}+n(\bar{\varepsilon}/BT)-BT]}, \quad 0 \le \varepsilon \le T , \tag{69}$$

where

$$\bar{\varepsilon} \triangleq B\varepsilon , \tag{70}$$

and we define the sampling function Sa(·) by

$$Sa(\xi) \triangleq \xi^{-1} \sin(\xi) . \tag{71}$$

Thus,

$$|C_n(\varepsilon)|^2 = \left(\frac{BT - \bar{\varepsilon}}{BT}\right)^2 Sa^2\left\{\pi(\bar{\varepsilon} - n)\left(\frac{BT - \bar{\varepsilon}}{BT}\right)\right\}$$

$$+\left(\frac{\bar{\varepsilon}}{BT}\right)^2 Sa^2\{\pi(\bar{\varepsilon} - n - BT)\bar{\varepsilon}/BT\}$$

$$+ 2\left(\frac{BT - \bar{\varepsilon}}{BT}\right)\left(\frac{\bar{\varepsilon}}{BT}\right) Sa\left\{\pi(\bar{\varepsilon} - n)\left(\frac{BT - \bar{\varepsilon}}{BT}\right)\right\} Sa\{\pi(\bar{\varepsilon} - n - BT)\bar{\varepsilon}/BT\} \tag{72}$$

$$\cdot \cos[\pi(BT - n)] , \qquad 0 \le \varepsilon \le T .$$

The first term in (72) has its largest amplitudes when $\bar{\varepsilon}$ is small; it peaks to largest values when $\bar{\varepsilon} = n$. If BT is reasonably large (say 20 or more) then the first term will be fairly small for $\bar{\varepsilon}$ near BT. The second term has its largest amplitude coefficient $(\bar{\varepsilon}/BT)^2$ when ε is near BT. However, since the argument of the sampling function is always negative (zero only for $\bar{\varepsilon} = BT$ and $n = 0$) for $n \ge 1$, the second term's total amplitude will tend to be small for all $\bar{\varepsilon}$ when $n \ge 1$. This fact also means the third term in (72) is small. Thus, for large BT,

$$|C_n(\varepsilon)|^2 \approx \left(\frac{BT - \bar{\varepsilon}}{BT}\right)^2 Sa^2\left\{\pi(\bar{\varepsilon} - n)\left(\frac{BT - \bar{\varepsilon}}{BT}\right)\right\}$$

$$\approx \left(\frac{BT - n}{BT}\right)^2 Sa^2\left\{\pi(\bar{\varepsilon} - n)\left(\frac{BT - n}{BT}\right)\right\}, \quad 0 < \bar{\varepsilon} < BT . \tag{73}$$

On substitution of (73) into (65) we have

$$E_{0n} \approx \frac{(BT - n)}{\pi(BT)^2} \int_{-n\pi(BT-n)/BT}^{\pi(BT-n)^2/BT} Sa^2(x)dx \approx \frac{BT - n}{(BT)^2}, \quad 1 \le n \le BT - 1$$

$$\approx 0, \qquad BT - 1 < n . \tag{74}$$

The power spectrum now becomes

$$S_{\omega_d}(\omega) \approx \frac{V_T^2 \lambda^2 G_{T_0}^2 G_{R_0}^2 \pi^2 a}{(4\pi)^3 h^2 \omega_{dh}^2 BT} |\omega| e^{-b\sqrt{\left(\frac{\omega_{dh}}{\omega}\right)^2 - 1}}$$

$$\cdot \left\{1 + 2 \sum_{n=1}^{BT-1} \left(1 - \frac{n}{BT}\right) \cos\left[n\omega_T \frac{2h}{c}\left(\frac{\omega_{dh}}{|\omega|} - 1\right)\right]\right\}, \quad |\omega| < \omega_{dh} \tag{75}$$

$$= 0, \qquad |\omega| > \omega_{dh} .$$

It can be shown that

$$2 \sum_{n=1}^{N} \left(1 - \frac{n}{N}\right) \cos(nx) = -1 + \frac{1}{N}\left[\frac{\sin(Nx/2)}{\sin(x/2)}\right]^2 \tag{76}$$

and (75) reduces to

$$S_{\omega_d}(\omega) \approx \frac{V_T^2 \lambda^2 G_{T_0}^2 G_{R_0}^2 \pi^2 a}{(4\pi)^3 h^2 \omega_{dh}} \cdot \frac{|\omega|}{\omega_{dh}} e^{-b\sqrt{\left(\frac{\omega_{dh}}{\omega}\right)^2 - 1}}$$

$$\cdot \frac{\sin^2\left[\frac{BT\omega_T h}{c}\left(\frac{\omega_{dh}}{|\omega|} - 1\right)\right]}{(BT)^2 \sin^2\left[\frac{\omega_T h}{c}\left(\frac{\omega_{dh}}{|\omega|} - 1\right)\right]} \operatorname{rect}\left(\frac{\omega}{2\omega_{dh}}\right), \tag{77}$$

where we define

$$\operatorname{rect}\left(\frac{\omega}{2W}\right) = 1, \quad |\omega| < W \tag{78}$$

$$= 0, \quad |\omega| > W ,$$

as usual. Now in general, if we define

$$\tau_h \triangleq 2h/c , \tag{79}$$

then for most systems $\tau_h << T$ and the argument of the denominator sine term in (77) is small for all $|\omega|$ near ω_{dh}. Finally, we have the approximation

$$S_{\omega_d}(\omega) \approx \frac{V_T^2 \lambda^2 G_{T0}^2 G_{R0}^2 \pi^2 a}{(4\pi)^3 h^2 \omega_{dh}} \cdot \frac{|\omega|}{\omega_{dh}} e^{-b\sqrt{\left(\frac{\omega_{dh}}{\omega}\right)^2 - 1}} \text{rect}\left(\frac{\omega}{2\omega_{dh}}\right) \cdot \text{Sa}^2\left\{\pi B \tau_h \left(\frac{\omega_{dh}}{|\omega|} - 1\right)\right\} . \tag{80}$$

The normalized value of (80) is plotted in figure 4 for $B\tau_h = 2$. The constant terrain curve presumes $b = 0$ while the other curve presumes $b = 1.4$. For comparison, figure 5 shows similar plots for $B\tau_h = 4$. Clearly, the power spectrum tends to spread as the system becomes closer to the scattering surface, for a given bandwidth B.

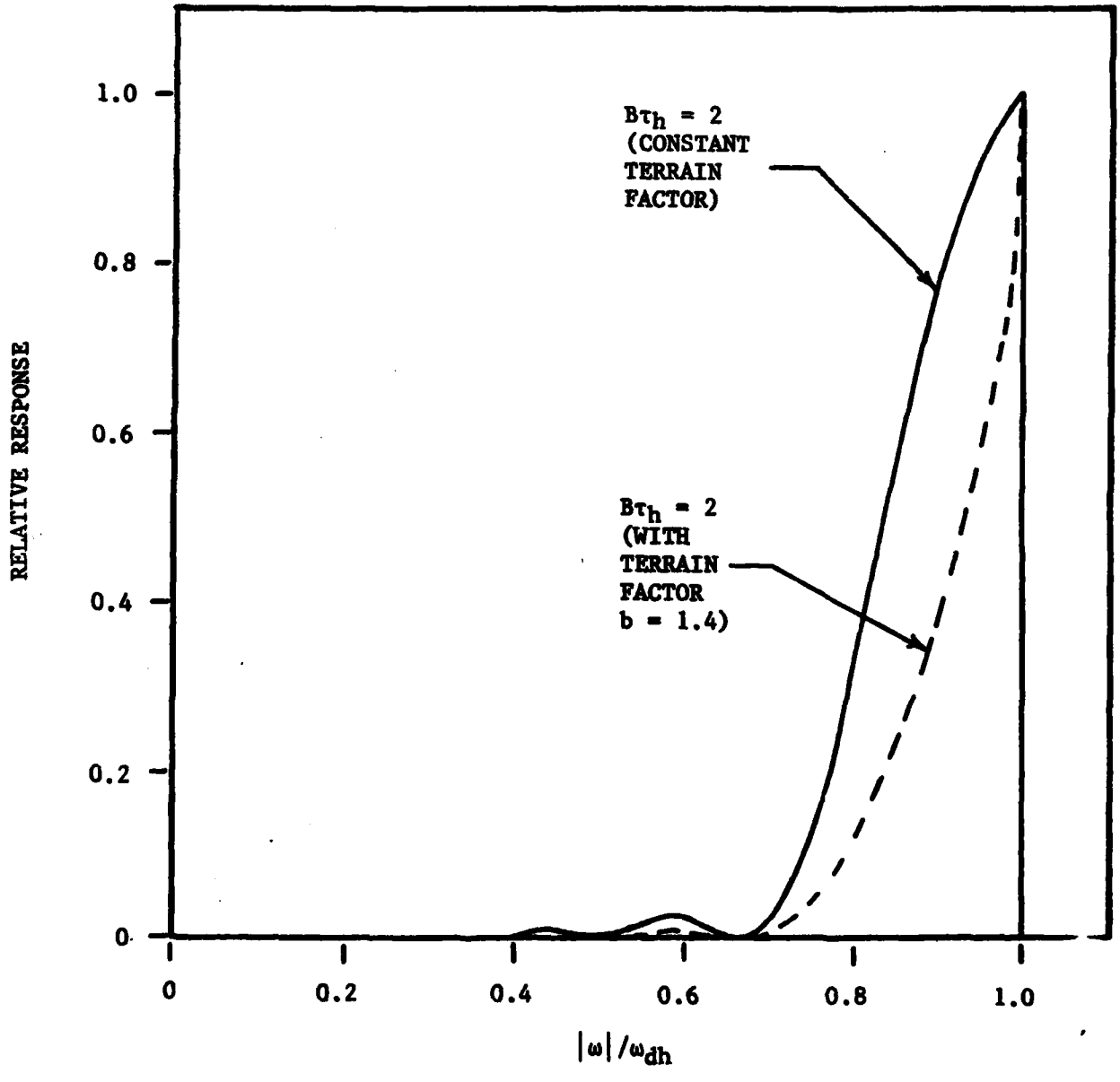

Figure 4. Normalized IF power spectrum $S_{\omega_d}(\omega)/S_{\omega_d}(\omega_{dh})$ as a function of frequency normalized to the vertical Doppler ω_{dh} for $B\tau_h = 2$.

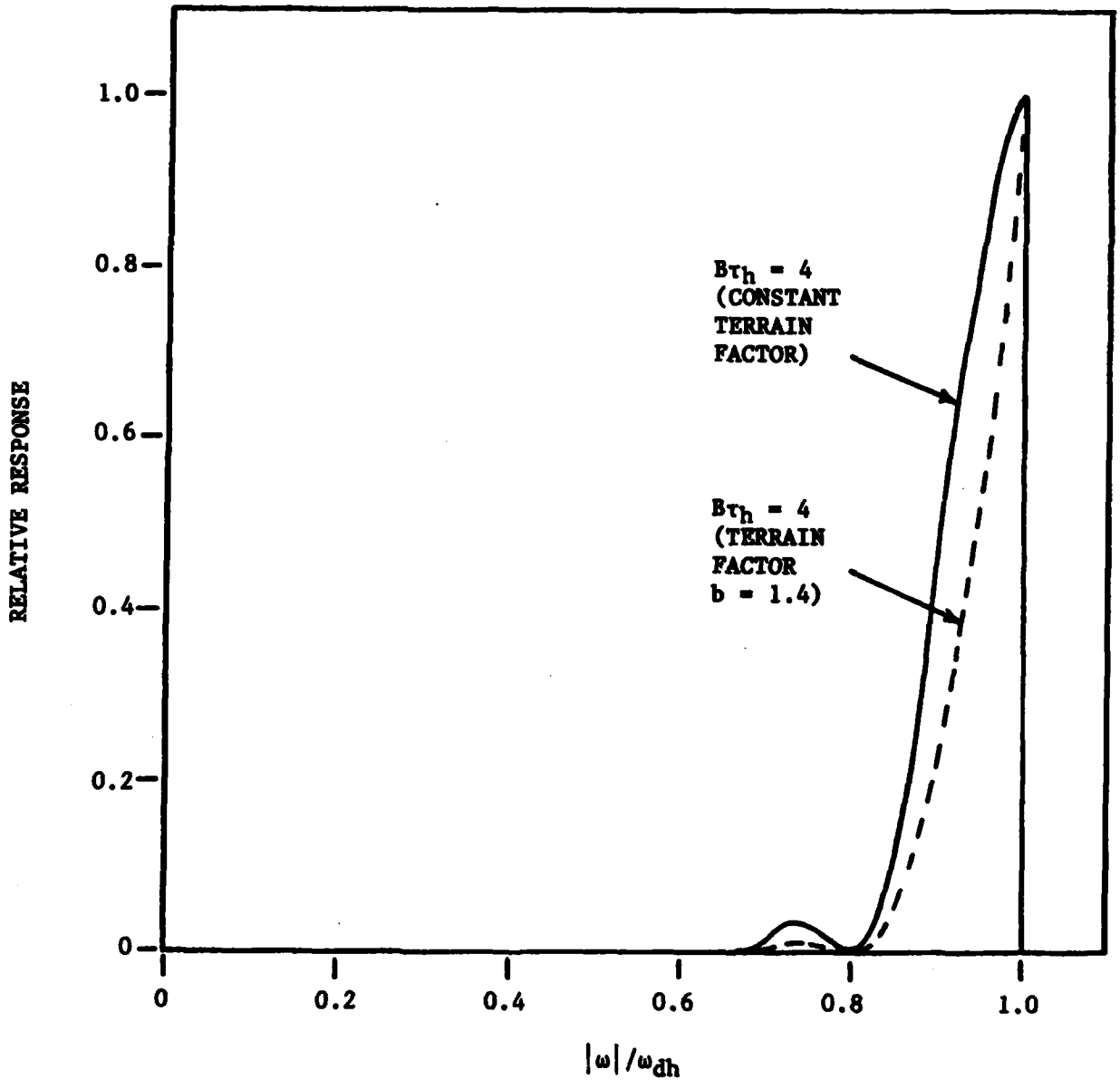

Figure 5. Normalized IF power spectrum $S_{\omega_d}(\omega)/S_{\omega_d}(\omega_{dh})$ as a function of frequency normalized to the vertical Doppler ω_{dh} for $B\tau_h = 4$.

APPENDIX

The steps leading from (52) to (63) are outlined in this appendix.

From well-known transforms[2] we first write (52) in the form

$$I_n(\omega) = \int_0^{\pi/2} \sigma_0(\theta) \cos\theta \sin\theta\, \pi e^{-jn\omega_T \frac{2h}{c}\left[\frac{1}{\cos\theta} - \frac{1}{\cos\theta_0}\right]} \delta(\omega - \omega_{dh}\cos\theta)\, d\theta$$

$$+ \int_0^{\pi/2} \sigma_0(\theta) \cos\theta \sin\theta\, \pi e^{jn\omega_T \frac{2h}{c}\left[\frac{1}{\cos\theta} - \frac{1}{\cos\theta_0}\right]} \delta(\omega + \omega_{dh}\cos\theta)\, d\theta \ .$$

Since θ can have values only from 0 to $\pi/2$ the impulse function in the first integral above will "occur" only for $0 < \omega < \omega_{dh}$. More precisely, it occurs when

$$\theta = \theta_1 = \cos^{-1}(\omega/\omega_{dh}).$$

For the values of ω for which the first term's impulse can occur, the second term's impulse cannot "occur" leading to the second integral above being zero for $0 < \omega < \omega_{dh}$. Similarly, the second term is nonzero for $-\omega_{dh} < \omega < 0$ while the first integral term is zero. When $|\omega| > \omega_{dh}$ neither impulses "occur" for any $0 < \theta < \pi/2$ and <u>both</u> integrals are zero. Hence $I_n(\omega) = 0$ for $|\omega| > \omega_{dh}$.

Consider the evaluation of the first integral above, which is nonzero only for $0 < \omega < \omega_{dh}$. Define

$$f(\theta) \triangleq \omega - \omega_{dh}\cos\theta$$

so

$$f'(\theta) \triangleq \frac{df(\theta)}{d\theta} = \omega_{dh}\sin\theta$$

$$|f'(\theta)| = |\omega_{dh}||\sin\theta| = \omega_{dh}\sin\theta$$

for $0 < \theta < \pi/2$. We apply a theorem of Friedman:[5]

---

[2] Peebles, Peyton Z, Jr., <u>Probability, Random Variables, and Random Signal Principles</u>, McGraw-Hill, 1980 (p. 256).

[5] Friedman, B., <u>Principles and Techniques of Applied Mathematics</u>, John Wiley, 1956 (Fifth printing, 1962) pp. 136-137.

Theorem If $\phi(x)$ is continuous at $x = x_0$ and $f(x)$ is a monotonic function of x that vanishes at $x = x_0$, then

$$\int_{-\infty}^{\infty} \phi(x)\delta[f(x)]dx = \frac{\phi(x_0)}{|f'(x_0)|} .$$

We identify θ with x, θ_1 with x_0, and apply the theorem to the first integral term in $I_n(\omega)$ by letting

$$\phi(\theta) \triangleq \sigma_0(\theta) \cos\theta \sin\theta \left\{ \pi e^{-jn\omega_T \frac{2h}{c}\left[\frac{1}{\cos\theta} - \frac{1}{\cos\theta_0}\right]} \right\} .$$

Thus,

$$I_n(\omega) = \frac{\pi\omega}{\omega_{dh}^2}\, \sigma_0\left[\cos^{-1}\left(\frac{\omega}{\omega_{dh}}\right)\right] e^{-jn\omega_T \frac{2h}{c}\left[\frac{\omega_{dh}}{\omega} - \frac{1}{\cos\theta_0}\right]} ,$$

for $0 < \omega < \omega_{dh}$.

By repeating the above procedure by letting $\omega = -|\omega|$ for $-\omega_{dh} < \omega < 0$ and identifying

$$\phi(\theta) = \sigma_0(\theta) \cos\theta \sin\theta \left\{ \pi e^{jn\omega_T \frac{2h}{c}\left[\frac{1}{\cos\theta} - \frac{1}{\cos\theta_0}\right]} \right\}$$

$$f(\theta) = -|\omega| + \omega_{dh} \cos\theta, \quad 0 < |\omega| < \omega_{dh}$$

$$\theta_1 = \cos^{-1}\left(|\omega|/\omega_{dh}\right)$$

$$f'(\theta_1) = -\omega_{dh} \sin\theta_1 ,$$

we develop the second integral for $I_n(\omega)$ as

$$I_n(\omega) = \frac{\pi|\omega|}{\omega_{dh}^2}\, \sigma_0\left[\cos^{-1}\left(\frac{|\omega|}{\omega_{dh}}\right)\right] e^{jn\omega_T \frac{2h}{c}\left[\frac{\omega_{dh}}{|\omega|} - \frac{1}{\cos\theta_0}\right]} ,$$

for $-\omega_{dh} < \omega < 0$.

By combining the above two results for $I_n(\omega)$ we obtain (63).

REFERENCES

[1] M. Abramowitz and I. A. Stegun (editors), Handbook of Mathematical Functions with Formulas, Graphs, and Mathematical Tables, Dover Publications, fifth printing corresponding to seventh (May 1968) printing by U. S. Government Printing Office except that corrections were made on 10 pages as noted on page II.

[2] Peyton Z. Peebles, Jr., Probability, Random Variables, and Random Signal Principles, McGraw-Hill, 1980.

[3] M. I. Skolnik, Introduction to Radar Systems, McGraw-Hill, 1962.

[4] M. I. Skolnik, Introduction to Radar Systems, 2nd Edition, McGraw-Hill, 1980.

[5] B. Friedman, Principles and Techniques of Applied Mathematics, John Wiley, 1956 (Fifth printing, 1962), pp. 136-137.

DISTRIBUTION

Administrator
Defense Technical Information Center
ATTN: DTIC-DDA (12 copies)
Cameron Station, Building 5
Alexandria, VA 22314

Harry Diamond Laboratories
ATTN: CO/TD/TSO/Division Directors
ATTN: Record Library, 81200
ATTN: HDL Libraty, 81100 (2 copies)
ATTN: HDL Library, 81100 (Woodbridge)
ATTN: Technical Reports Branch, 81300
ATTN: Chairman, Editorial Committee
ATTN: Legal Office, 97000
ATTN: Chief, 11400 (10 copies)
2800 Powder Mill Road
Adelphi, MD 20783

END

FILMED

3-83

DTIC